Temporal Complexity Measure of Reaction Time Series: Operational vs. Chronological Time

Korosh Mahmoodi (koroshmahmoodi@gmail.com)
United States Army Research Laboratory
Scott E. Kerick
United States Army Research Laboratory
Paolo Grigolini
University of North Texas
Bruce J. West
University of North Texas
Piotr J. Franaszczuk
Johns Hopkins University School of Medicine

Article

Keywords:

Posted Date: May 12th, 2022

DOI: https://doi.org/10.21203/rs.3.rs-1617624/v1

Temporal Complexity Measure of Reaction Time Series: Operational vs. Chronological Time

Korosh Mahmoodi[1,2,*], Scott E. Kerick[1], Paolo Grigolini[2], Bruce J. West[2], and Piotr J. Franaszczuk[1,3]

[1]US Combat Capabilities Command,Army Research Laboratory, Aberdeen Proving Ground, MD 21005, USA
[2]Center for Nonlinear Science, University of North Texas, P.O. Box 311427, Denton, TX 76203, USA
[3]Department of Neurology, Johns Hopkins University School of Medicine, Baltimore, MD 21287, USA
[*]koroshmahmoodi@gmail.com

ABSTRACT

Detrended Fluctuation Analysis (DFA) is a well-known method to evaluate scaling indices of time series, categorizing the dynamics of complex systems. In the literature, DFA has been used to study the fluctuations of reaction time RT(n) time series, where n is the trial number. Herein we propose treating each RT(n) as a duration time that changes the representation from operational (trial) time n to chronological (temporal) time t, or RT(t). To do this, we fill each time interval of RT(n) with fixed noise of magnitude 1 and with a randomly determined sign. The fixed noise represents the rigidity (order) and the random change of sign represents the flexibility (randomness) of the generated time series RT(t). Then the DFA algorithm was applied to RT(t) time series to evaluate scaling indices. We show that this new perspective leads to better results in: 1) differentiating scaling indices between low vs. high time-stress conditions and 2) predicting task performance outcomes. The dataset we analyzed is based on a Go-NoGo shooting task which was performed by 30 participants under low and high time-stress conditions in each of six repeated sessions over a three week period.

Introduction

Reaction time (RT) time series, where n is the trial number (RT(n)), has been a hallmark measure of perceptual-motor and cognitive performance for more than a century[1,2]. Typically, RT(n) time series have been analyzed based on statistical moments of the distribution of sequences of trials in various experimental conditions (mean, variance, skewness, kurtosis). However, this approach fails to capture the underlying dynamics of the intermittent fluctuations inherent in RT(n), which are central to modeling neural latency mechanisms at a macroscopic scale[1,3]. Previous RT(n) research reveals inverse power law statistics ($1/f$ scaling is interpreted to be long-range temporal correlations) in cognitive and behavioral time series data[4–11].

Researchers have shown that individuals performing more difficult tasks requiring greater cognitive effort exhibit relatively lower scaling indices of RT(n) time series than those observed for simpler tasks. For example, in a series of experiments Kello et al.[8] found lower scaling indices for variable versus fixed trial intervals, random versus patterned cues, and unpreviewed versus previewed trials. Similarly, Correll[4] found lower scaling indices in participants who reported high effort to avoid racial bias while responding to black versus white target stimuli under threat/no threat conditions (see also Grigolini et al.[7] for a theoretical explanation). In a similar Go-NoGo paradigm, Simola et al.[10] showed that scaling indices were inversely related to cognitive flexibility, as measured by errors of commission (i.e., by higher scaling indices associated with lower errors). Wijnants et al. (2009)[11] showed that a scaling indices becomes steeper (more clearly patterned 1/f) as participants become more skilled in a precision-aiming motor task over blocks of practice. Overall the evidence suggests that higher scaling indices are reflective of higher levels of cognitive and behavioral performance and/or performance of simpler tasks.

In this work the existence of power law scaling indices were examined using data previously recorded during a Go-NoGo shooting task under low and high time-stress conditions as part of a neurofeedback training study (See Task and Procedures below, and Spangler et al.[12] and Kerick et al.[13] for more details). We are not aware of previous research which has investigated the effects of time-stress on scaling indices over different timescales within and across repeated experimental sessions spanning several days or weeks. The study examined the effects of time-stress with shorter (high stress) and longer (low stress) time allocated for the task (i.e., target exposure durations) as well as changes with practice over six sessions. The shooting task required the participants to scan the environment for targets appearing over spatially-distributed locations, detect and orient the weapon toward the target upon its appearance, identify whether the target is friend or foe, decide whether to shoot or not, and if the decision is to shoot, the participant must aim and fire the weapon within the constrained time interval in which the target is exposed. As a task designed to assess inhibitory executive control mechanisms by evaluating errors of commission (shots fired

at friendly targets), this shooting task variant represents a more ecologically-valid, complex and challenging Go-NoGo task than has been implemented in previous research. Typically, Go-NoGo tasks consist of stimuli appearing on a computer screen in a fixed location, and Go responses are simple button presses on a keyboard[4,10]. We also have a relatively small number of trials in each condition in each session ($n = 360$) because the previous study was structured to limit overall length of the experiment, which could introduce additional effects of boredom or fatigue. Thus, these data present a challenge for rigorous testing of theoretical models and analytical approaches for identifying power laws and scaling from shorter time series generated under more complicated task conditions than in previous applications.

Because of the relatively short RT(n) time series of our dataset, the previously established methods do not provide reasonable estimates of the power law index. The scaling index in previous studies is typically estimated by finding the slope of a linear approximation to the power spectral density (PSD) function in log-log coordinates. The PSD estimate is usually achieved by applying the fast Fourier transform (FFT) to the RT trial series (1:N), which requires a relatively large number of stationary data points to obtain low variance and stable PSD estimates. Typically, researchers implement tasks consisting of 1000 or more trials to enable stable spectral estimates, and the evolution of longer periods to observe slow fluctuations, although as few as 200 trials have been employed[4]. Because the power law selection of interest in PSD occurs at low frequencies, we need to have long time series to obtain meaningful power law behavior for at least one decade of frequency. As such, short time series create noisy PSD estimates, and consequently power laws of uncertain slope.

Detrended Fluctuation Analysis (DFA) has also been widely used to measure the scaling indices of RT(n) time series[10,11,14]. In previous studies, the signal analyzed by DFA has been the RT(n) time series measured at each trial n of the experiments. This represents a time series expressed in trial intervals referred to as operational time[15]. For simple tasks power law relations have been found using PSD or DFA[4,5,8,10], but as we show herein, for RT(n) of a more realistic task with short trial sequences, the PSD or DFA might not be able to extract a reliable measure of the scaling indices of the process.

In this work, we propose a new point of view by considering each RT(n) as a time interval (RT(t) in ms) and filling each interval with a fixed noise (of magnitude 1 and a random sign). This represents a latency or duration time series expressed in temporal intervals referred to as chronological time[15]. This secondary time series, which we call RT(t), represents the rigidity (constant noise) and flexibility (changing sign) of the process. By measuring the complexity of the RT(t) time series, using DFA, we found a clear classification of scaling indices between low and high time-stress conditions. We also found clear trends between scaling indices and errors of commission. Neither of these findings were observed for the traditional DFA analysis of RT(n) time series.

To connect the scaling index α of the RT(t) time series, measured by DFA, to the temporal complexity index, we used simulated RT(n) time series, with an inverse power law (IPL) probability density function (PDF) having a IPL index μ, generated using the well-known Manneville map[16]. Then, we created the corresponding simulated RT(t) time series and measured their α via DFA. Consequently, we found the relationship between α and μ, making it possible to connect α to the power-law index of the PSD.

Results

Wilcoxon Matched-Pairs Signed Rank Tests of Differences between Time-Stress Conditions for Errors of Commission and DFA Scaling Indices

Wilcoxon matched-pairs signed rank tests applied to errors of commission and DFA scaling indices of RT(n) and RT(t) time series for individual sessions revealed statistically significant differences for errors of commission (Z = -4.5560; p. < .001) and RT(t) (Z = 4.7821; p. < .001), but not for RT(n) (Z = -0.1954; p. = .85). For all sessions appended, statistically significant differences were observed for errors of commission (Z = -9.3265; p. < .001) and RT(t) (Z = 11.0996; p. < .001), but not for RT(n) (Z = -0.3871; p. = .70). Table 1 provides median and quantile (.25 .75) values for each dependent variable under each time-stress condition. Figure 1 shows differences of scaling indices between low and high time-stress conditions for DFA analysis of RT(n) and RT(t) time series. The DFA analysis of RT(t) time series could categorize the scaling indices of the two conditions.

Next, we evaluated whether shuffling the RT time series prior to DFA analysis destroys the long term correlations inherent in the intact RT time series and lowers scaling indices. Figure 2 compares the DFA applied to randomly shuffled RT(n) and RT(t) time series. After shuffling, the DFA analysis of RT(n) time series gave scaling indices close to $\alpha = 0.5$ (randomness), while in the case of DFA analysis of RT(t) time series, shuffling does not significantly change scaling indices.

Regression Analyses of DFA Scaling Indices for Predicting Errors of Commission

Regression analyses revealed that scaling indices derived from DFA analysis of RT(n) time series was not a significant predictor of errors of commission in either low or high time-stress conditions for either individual sessions or all sessions appended (all ps > .05; see Table 2). However, scaling indices derived from the DFA analysis of RT(t) time series were all highly significant

Table 1. Median and Quantile (.25 .75) Values by Time-Stress Condition

Var	Low	High
Individual Sessions		
Errors	0.17 (0.11 0.22)	0.33 (0.24 0.48)
RT(n)	0.62 (0.58 0.64)	0.62 (0.59 0.65)
RT(t)	0.75 (0.72 0.78)	0.71 (0.68 0.72)
All Sessions Appended		
Errors	0.15 (0.08 0.28)	0.33 (0.19 0.50)
RT(n)	0.59 (0.51 0.65)	0.60 (0.52 0.66)
RT(t)	0.75 (0.71 0.77)	0.69 (0.67 0.72)

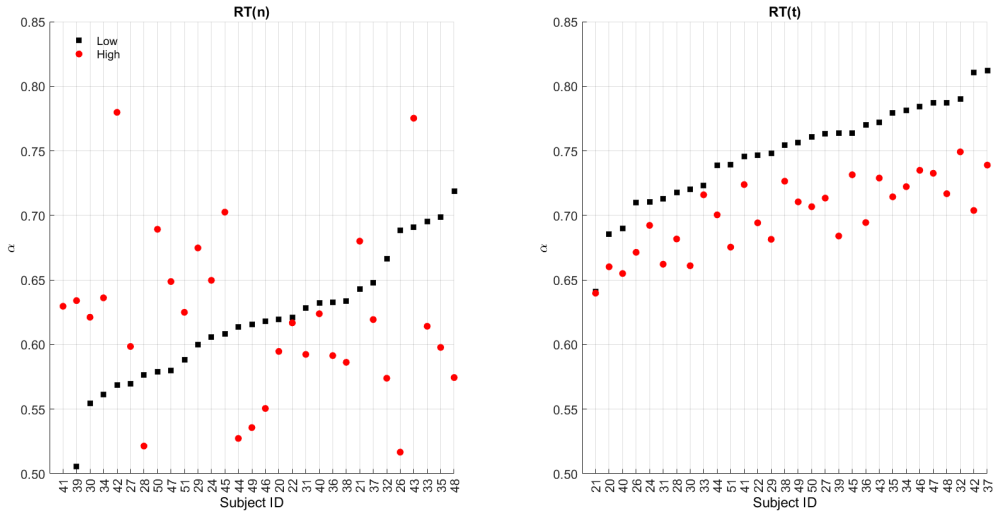

Figure 1. Left panel: scaling indices measured by DFA analysis of the RT(n) time series of participants in high (red dots) and low time-stress (black squares) conditions. Right panel: scaling indices measured by DFA analysis of the RT(t) time series of each participant in high (red dots) and low time-stress (black squares) conditions. Paired data are sorted by indices in low time-stress condition in both panels. Each data point is averaged over 100 DFA analyses of RT(t) time series.

(all ps < .001; see Table 3). Higher scaling indices were associated with lower errors of commission. Further, the associations were stronger for data in the high vs. low time-stress condition.

Figures 3 and 4 show the errors of commission vs. scaling indices α, measured via DFA processing of RT(n) and RT(t) datasets, respectively. In each figure the top and bottom panels correspond to the data of individual sessions and appended sessions, respectively. Also, the left panels and right panels are data from low and high time-stress conditions, respectively. As can be seen, the DFA processing of RT(n) time series did not reveal any interdependence between the errors of commission of the participants and their value of scaling index (Figure 3). On the other hand, using DFA to process the corresponding RT(t) time series shows a clear trending; participants with higher values of the scaling index have lower errors of commission (Figure 4).

Discussion

We developed and applied a new approach to measuring the scaling index of reaction time series data using DFA, from a short, complex cognitive-motor decision making task. In this method we consider each reaction time as a duration time and create a secondary time series RT(t) by filling each time interval with fixed noise of magnitude 1 and a random sign and measured its scaling index using DFA. The RT(t) time series represents the rigidity/flexibility of the process. Using the new method we were able to show the existence of relations between scaling indices and errors of commission, a measure of cognitive flexibility (consistent with Simola[10]), while traditional DFA processing of RT(n) time series failed to show any such relation. Although Simola[10] observed power-law scaling of RT(n) time series from a Go-NoGo task using autocorrelation functions, PSD, and DFA, their task consisted of 1000 equally spaced trials and was presented on a computer monitor requiring keyboard

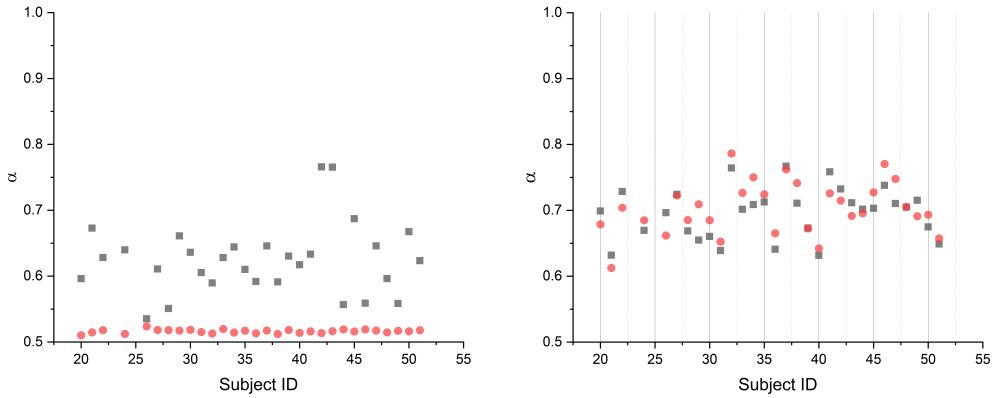

Figure 2. The left panel shows the results of applying DFA to the RT(n) time series (black squares) and to shuffled RT(n) time series (red dots). The right panel depicts the results of applying DFA to RT(t) time series (black squares) and to shuffled RT(t) time series (red dots).

Table 2. Regression Analyses of RT(n) Scaling Indices Predicting Errors of Commission

Coeff	Estimate	SE	t	p	Adj R^2
Individual Sessions					
(Intercept)	0.27	0.21	1.32	0.20	
Beta Low	-0.14	0.34	-0.42	0.68	-0.0293
(Intercept)	0.35	0.30	1.18	0.25	
Beta High	0.01	0.48	0.02	0.99	-0.0357
All Sessions Appended					
(Intercept)	0.18	0.06	3.02	0.003	
Beta Low	0.02	0.10	0.19	0.85	-0.00553
(Intercept)	0.35	0.09	3.73	0.0003	
Beta High	0.02	0.16	0.11	0.92	-0.00585

responses. These two methodological differences (lower trial numbers and greater task complexity) may account for why we did not observe power-law scaling of RT(n) time series in the present study. Further, the new method of DFA processing of RT(t) time series was able to discriminate between low and high time-stress conditions, whereas DFA analysis of RT(n) time series was not. Our finding by applying DFA to RT(t) time series is also consistent with previous research which has observed higher scaling indices in RT(n) time series associated with lower task demand or decreased task complexity with longer trial series (>1000)[8] (see also[14]).

The stronger negative relation between scaling indices and errors of commission in the high time-stress condition suggests that under higher time demand conditions, it is beneficial for the system to shift from a more ordered, predictable state to a more disordered, unpredictable state. However, a shift too far in this direction toward disorder results in deterioration of inhibitory control. Lower scaling indices in the high vs. low time-stress condition suggests that behavior is more disordered or unpredictable (more random) in the high time-stress condition, an effect which appears to be environmentally coupled to the time constraints imposed by the task. Together, these two findings support previous research suggesting that system complexity is associated with greater degrees of freedom, thus facilitating greater flexibility and adaptability of the system to internal and external perturbations or task demand conditions[8,9,11,17,18].

Traditional DFA provides a method to quantify long-range correlations in time series and to index repeating patterns over different time scales[19]. As our results reveal, randomly shuffling the RT(n) time series destroys the temporal structure of the time series which results in scaling indices around 0.5. However, applying DFA to the shuffled RT(t) time series results in scaling indices compatible with those obtained from the intact RT(t) time series. This result suggests that the DFA analysis of RT(t) time series provides a method for detecting crucial events (i.e., renewal processes), which are temporally uncorrelated[15], but cannot infer long-range temporal correlations. The results of shuffling analysis show that RT(t) time series, unlike the traditionally used RT(n) series, is not at all sensitive to different intervals between trials. In our experiment the intervals within

Table 3. Regression Analyses of RT(t) Scaling Indices Predicting Errors of Commission

Coeff	Estimate	SE	t	p	Adj R^2
Individual Sessions					
(Intercept)	1.24	0.17	7.32	$8.83 * 10^{-12}$	
Beta Low	-1.41	0.23	-6.20	$3.92 * 10^{-9}$	0.177
(Intercept)	2.71	0.28	9.69	$6.99 * 10^{-18}$	
Beta High	-3.37	0.40	-8.42	$1.67 * 10^{-14}$	0.295
All Sessions Appended					
(Intercept)	1.34	0.28	4.77	$5.19 * 10^{-5}$	
Beta Low	-1.53	0.37	-4.11	$3.17 * 10^{-4}$	0.353
(Intercept)	2.96	0.57	5.16	$1.81 * 10^{-5}$	
Beta High	-3.71	0.82	-4.54	$9.76 * 10^{-5}$	0.403

sessions were randomly distributed and there were longer intervals between sessions, but due to this property of the method we could concatenate trials even when temporal distance between trials differ significantly (e.g. between sessions). This will make the method suitable for even more realistic experimental and real-world conditions where intervals between responses to stimuli may vary significantly. In other words, the statistics are renewal, and the events are statistically independent of one another. Shuffling the time series will not change the statistics, so they will again be an IPL with index μ. Now we consider a second time series to which we apply DFA and get a scaling index λ. But we know when we shuffle the time series, we are going to obtain a different scaling index, say α, because the index λ we obtained had to do with long-range correlations that are destroyed when we shuffle. If the second time series (before shuffling) is fractional Brownian motion (FBM) then we would obtain $\alpha = 0.5$. However, if the time series is mixed, we could obtain $\alpha = \mu$ so that the shuffling acts like a filter and the deviation of α from 0.5 is that part of the mixed time series that is renewal.

We note that the method of subordination to ordinary diffusion proposed by Sokolov et al.[20] to illustrate the popular theory of Continuous Time Random Walk (CTRW)[21] is widely adopted to generate the events that are the source of temporal complexity revealed by the statistical analysis of experimental data. For instance, the authors of[15] used this theoretical interpretation to describe the temporal complexity of individuals of a decision making social system. Subordination makes it possible to convert the fluctuations of data that would not generate a departure from ordinary diffusion into rare events yielding temporal complexity. Our new method is based on converting the intensity (latency) of reaction times as a function of chronological time (see the left panel of Figure 6) into the time intervals between two consecutive events. The time interval between two consecutive events is filled with either +1 or -1, tossing a fair coin. In[22] this approach was used to illustrate the anomalous diffusion properties of events, with a waiting-time PDF known to be proportional to $1/\tau^{\mu}$ with τ denoting the time interval between two consecutive events. However, in this paper, the number of reaction times available to us is not large enough to allow us to determine with precision the power law index μ from the distribution of the reaction times. We have directly converted the reaction times in the chronological order into a diffusion process without finding a deviation from ordinary scaling. Quite surprisingly we found that the adoption of the velocity model, used for the first time to the best of our knowledge, to detect the complexity of the experimental fluctuations allows us to evaluate with precision the parameter μ.

Methods

Participants

Thirty ($N = 30$; 13 female) young healthy adults (ages 18-40 yr; mean 24.99 ±3.21) participated in six separate sessions within a three-week interval. Volunteers who agreed to participate were asked to read and sign an Informed Consent Agreement (approved by the Human Use Committee at the US Army Research Laboratory and the Institutional Review Board at the University of Maryland, Baltimore County, in accordance with the Declaration of Helsinki and the U.S. Code of Federal Regulations).

Task design

The Go-NoGo task was implemented in virtual reality using HTC Vive (https://www.vive.com/us/). In each session, the participants completed four blocks of 90 trials (360 total trials) in each low and high time-stress condition (2160 total trials in each condition over six sessions). Pop-up targets were pseudo-randomly distributed 40 times at each of 9 range locations (three simulated distances (near, mid, far) by three lanes (left, center, right) and exposed at variable onset intervals (1000 ± 500 ms over a Gaussian-distributed range of 100 ms increments) for various target exposure durations (see Figure 5). The probability of targets (enemy; red) to non-targets (friendly; green) was .90/.10, respectively to induce a prepotent response bias.

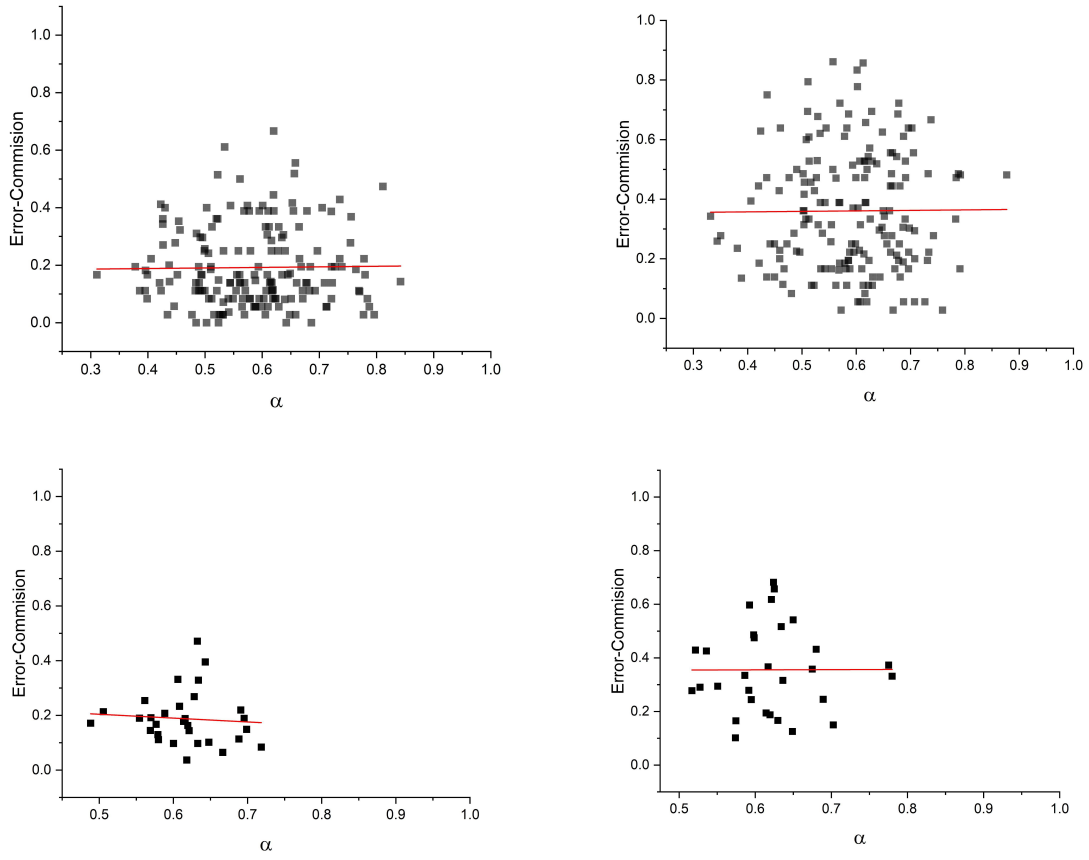

Figure 3. The figures show the errors of commission vs. scaling indices of DFA on RT(n)s of all sessions of all participants (top figures) and appended sessions of all the participants (bottom figures) for two cases of low (left figures) and high time-stress conditions (right figures).

The participants were instructed to "shoot enemy targets as quickly and accurately as possible, while refraining from shooting at friendly targets". Time-stress conditions were individualized based on a pre-testing performance thresholding procedure to account for individual differences in participants' ability to perform the task. This was done by empirically determining target exposure durations corresponding to the 50th (high time-stress) and 90th (low time-stress) percentile hit-rates in response to 100 enemy targets using psychophysical methods (method of limits[23]). Figure 5 provides example RT time series from a representative subject in low and high time-stress conditions in one session. Herein we analyze scaling index of RT times series and examine their relation to the performance measure errors of commission, defined as shots fired at friendly targets (incorrect committed responses).

Data Analysis

Across all subjects, sessions, and conditions, 122153 raw RT trials were first pruned of extreme latency values (100 ms < RT < 1500 ms). This resulted in removal of 659 RT trials (121494 preserved for subsequent analysis). After trimming the data of outliers, we proceeded with DFA analyses of RT(n) and RT(t), each at the single session time scale (360 trials) and across all six sessions concatenated (2160 trials). We also simulated RT(n) and RT(t) time series consisting of temporal complexity consistent with our empirical observations at each time scale.

DFA analysis of RT(n) time series

For each subject under each condition and time scale, we computed the percentage of errors of commission and applied DFA analyses to RT(n) time series. DFA is applied to reveal long-range correlations in time series[19]. The method consists of (1) integrating the time series (1:N samples), (2) dividing the integrated time series into windows of length n, (3) deriving least

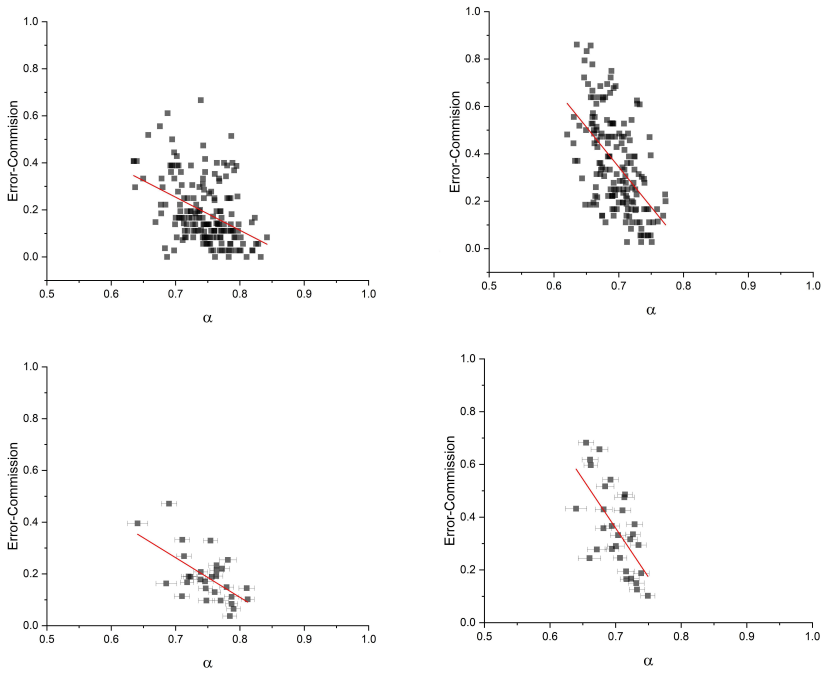

Figure 4. The figures show the trend between the errors of commission and scaling indices of DFA analysis if RT(t) time series of all sessions of all participants (top figures) and appended sessions of all the participants (bottom figures) for two cases of low (left figures) and high time-stress conditions (right figures). Each data point is averaged over 100 DFA on RT(t)s.

squares line of fit to the data in each window, (4) subtracting the linear trend from each window, and (5) calculating the root mean square amplitude in each window:

$$F(n) = \sqrt{\frac{1}{N}\sum_{k=1}^{N}[y(k) - y_n(k)]^2}$$

This process is repeated over time scales (window lengths from n=4 to n=N/2) to determine the relationship between the average fluctuation, F(n), and window length, n. The scaling exponent is then determined by estimating the slope of the line relating F(n) to n plotted on a log-log scale.

DFA analysis of RT(t) time series

Figure 6 shows a schematic for transforming data from operational time (RT(n)) to chronological time (RT(t). The left panel of this figure shows some data points in trial time n, X(n). In the right panel each of these data points is used as a latency time, and filled with +1 or -1, chosen randomly. For real datasets of RTs, the RTs were first rounded to three significant digits (in ms) and the resulting RT(t) time series was processed using DFA and the corresponding scaling index α calculated. Notice that such a generated RT(t) time series has a random component (i.e. the sign of each duration time), so, we can make many different RT(t) time series. To consider all the possibilities, for each RT(n) time series we ran DFA over 100 generated RT(t) time series and evaluated the average value of α.

Comparing the DFA of RT(n) and RT(t)

Figure 7 shows the differences in the DFA graph when RT(n) time series of an individual was used (left panels) vs. the DFA graph on its corresponding RT(t) (right panels). The RT(n) were taken from a representative participant in one session (top panels) and across all six sessions appended (bottom panels), in the low time-stress condition. As can be seen in the figure, the DFA graph of the RT(t) has fewer fluctuations and a more extended power-law domain.

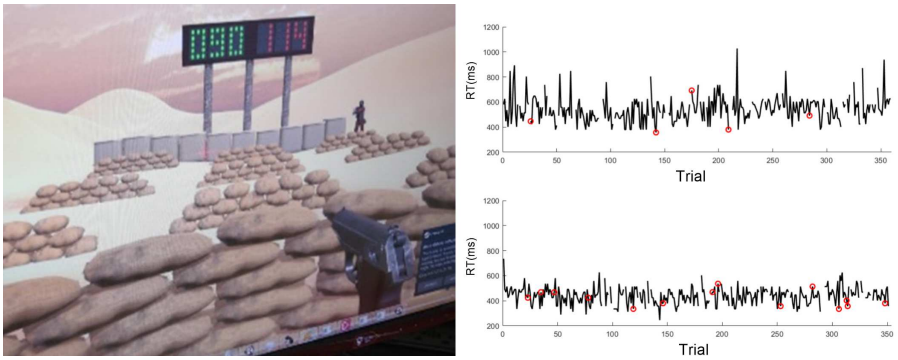

Figure 5. Left panel: Virtual reality Go-NoGo shooting task via participant's first-person perspective in HTC Vive. Right panel: Example participant's RT trial series in low (top) and high (bottom) time-stress conditions. Red circles indicate errors of commission, gaps in time series indicate lack of trigger responses on those particular trials (i.e. correct omissions to friendly targets or errors of omission to enemy targets).

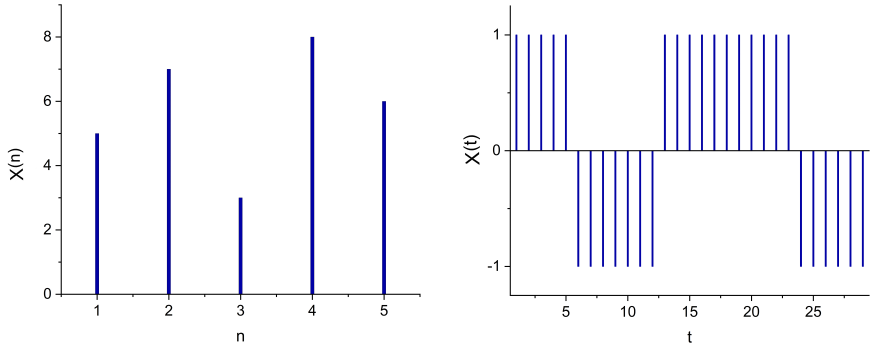

Figure 6. The schematics of changing data from operational time X(n) (left panel) to chronological time X(t) (right panel.) Each data point in operational time X(n) is considered as a duration time and filled with +1 or -1, assigned randomly (in this example each latency interval is filled with +1, -1, +1, +1, and -1, respectively). Notice that because of the random assignment of signs, there are many possible X(t)s. To consider this variety, especially for short time series, we should use an ensemble average for our analysis.

DFA on simulated reaction times with different temporal complexity μ

To introduce the method used herein, and relating temporal complexity to scaling measured by DFA, we used simulated data, temporally complex, using turbulence intermittency as prescribed by Mannevillle[16]. In order to make the numerical generation of the events faster, we adopted an idealized version of this map in the following[24] way: each RT can be calculated by transforming the sequence y_i of random numbers uniformly distributed in the interval (0, 1) into the sequence τ_i :

$$\tau_i = T \frac{1}{y_i^{\frac{1}{\mu-1}} - 1}, \tag{1}$$

where μ ($\mu > 1$) is the temporal scaling index of the generated time series. The τ's are generated by a PDF $\psi(\tau)$ defined by:

$$\psi(\tau) = (\mu - 1)\frac{T^{(\mu-1)}}{(\tau + T)^{\mu}}, \tag{2}$$

which is properly normalized. The time constant T defines the time necessary to turn microscopic dynamics into a process with an evident IPL index μ. For $1 < \mu < 3$ this PDF represents a complex system. For $\mu > 3$ the dynamics falls into the region of normal statistics[25] and is no longer complex. We take the set of τ_i generated by the Manneville map, with a given scaling index

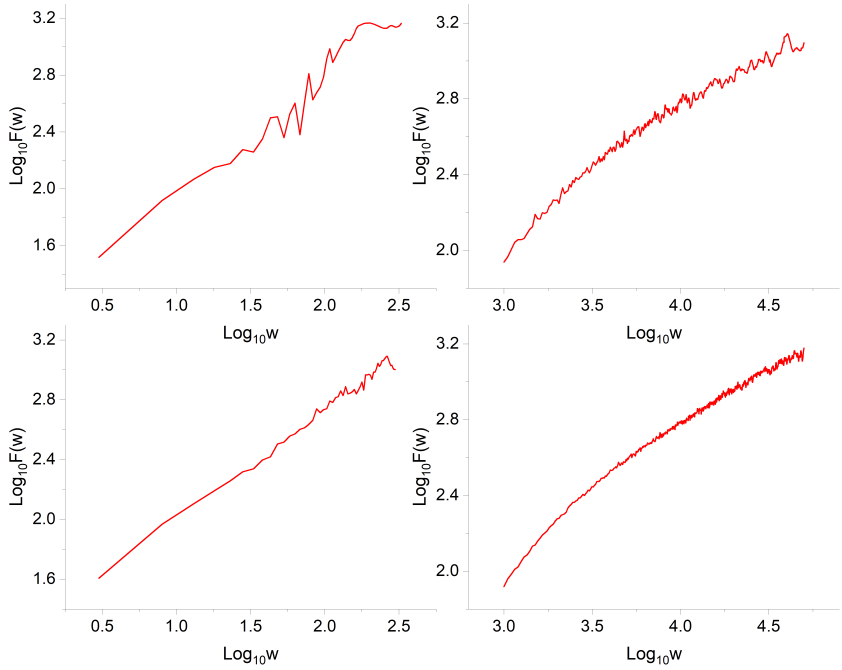

Figure 7. The left panels show the graph for DFA on the RT(n) time series of one participant during an individual session (top-left) and during all sessions appended (bottom-left). The right panels show the graph for DFA on the corresponding RT(t) time series (created according the description in Figure 6) of the same participant during an individual session (top-right) and during all sessions appended (bottom-right).

μ, as the simulated reaction times RT(n) and create the corresponding RT(t) time series. The DFA was then used to process the RT(t) time series (RT(t) generated using the prescription in Figure 6).

Figure 8 shows the resulting relationship between temporal complexity index μ of simulated time series and the scaling index α evaluated using DFA analysis of RT(t) time series. The linear fit can be approximated using:

$$\mu = 4 - 2\alpha. \tag{3}$$

So, this method is an indirect way of evaluating the temporal complexity index μ of short time series.

Relation between α and $1/f$ noise

Here we connect the scaling index α measured via DFA processing of RT(t) time series to the power-law index of $1/f^m$ noise. It is known that the series of events created by the Manneville map with scaling index μ has an IPL PDF[26]:

$$S(f) \propto 1/f^m \propto 1/f^{(3-\mu)}. \tag{4}$$

Substituting the relation between index given by equation 3 into this expression we obtain:

$$S(f) \propto 1/f^{2\alpha-1}. \tag{5}$$

So, $\alpha = 1$ corresponds to a perfect $1/f$ noise.

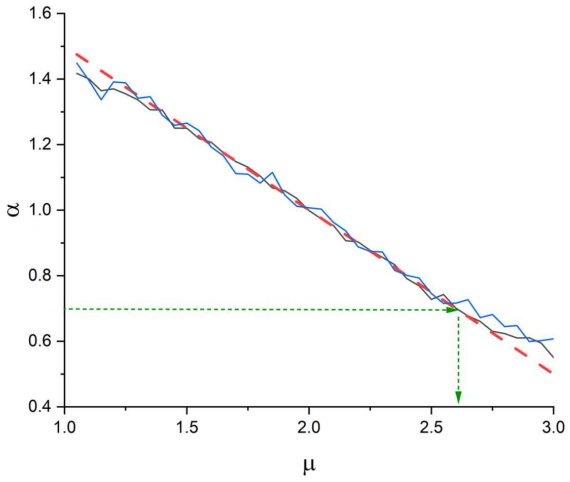

Figure 8. The DFA of simulated reaction time series. Each RT(n) is a duration time generated by the idealized Manneville map of reference[24] with corresponding temporal complexity index (μ). The RT(n) time series used to generate the corresponding RT(t) time series using the description of Figure 6. The length of the simulated RT(t) time series were chosen to be similar to the RT(t) dataset in the session level (blue line) and the appended sessions (black line). The dotted red line is the linear fit (equation 3). The dotted green lines show an example of estimating the temporal complexity index μ from measured α using DFA applied to RT(t) time series.

Statistical analysis

Wilcoxon matched-pairs signed rank tests were applied to determine whether errors of commission and values of the scaling index for the two DFA analyses differed between low and high time-stress conditions at each time scale. Separate linear regression analyses were also applied using values of the scaling index (DFA processing of RT(n) and RT(t)) as predictors and errors of commission as response outcomes under each condition and time scale to determine whether the strength of the predictors differed between conditions.

Data availability

The datasets used and/or analysed during the current study available from the corresponding author on reasonable request.

References

1. Luce, R. D. *et al. Response times: Their role in inferring elementary mental organization*. 8 (Oxford University Press on Demand, 1986).
2. Meyer, D. E., Osman, A. M., Irwin, D. E. & Yantis, S. Modern mental chronometry. *Biol. psychology* **26**, 3–67 (1988).
3. Smith, P. L. & Ratcliff, R. Psychology and neurobiology of simple decisions. *Trends neurosciences* **27**, 161–168 (2004).
4. Correll, J. 1/f noise and effort on implicit measures of bias. *J. personality social psychology* **94**, 48 (2008).
5. Gilden, D. L. Cognitive emissions of 1/f noise. *Psychol. Rev.* **108**, 35–56, DOI: https://doi.org/10.1037/0033-295X.108.1.33 (2001).
6. Gilden, D. L., Thornton, T. & Mallon, M. W. 1/f noise in human cognition. *Science* **276**, 1837–1839, DOI: https://doi.org/10.1126/science.7892611 (1995).
7. Grigolini, P., Aquino, G., Bologna, M., Lukovic, M. & West, B. J. A theory of 1/f noise in human cognition. *Phys. A* **388**, 4192–4204, DOI: https://doi.org/10.1016/j.physa.2009.06.024 (2009).
8. Kello, C. T., Beltz, B. C., Holden, J. G. & Van Orden, G. C. The emergent coordination of cognitive function. *J. Exp. Psychol. Gen.* **136**, 551–568, DOI: https://doi.org/10.1037/0096-3445.136.4.551 (2007).
9. Kello, C. T. *et al.* Scaling laws in cognitive sciences. *Trends Cogn. Sci.* **14**, 223–232, DOI: https://doi.org/10.1016/j.tics.2010.02.005 (2010).

10. Simola, J., Zhigalov, A., Morales-Muñoz, I., M., P. J. & Palva, S. Critical dynamics of endogenous fluctuations predict cognitive flexibility in the go/nogo task. *Sci. Reports* **7**, 2909, DOI: https://doi.org/10.1038/s41598-017-02750-9 (2017).

11. Wijnants, M. L., Bosman, A. M. T., Hasselman, F., Cox, R. F. A. & Van Orden, G. 1/f scaling in movement time changes with practice in precision aiming. *Nonlinear Dyn. Psychol. Life Sci.* **13**, 79–98 (2009).

12. Spangler, D. P. *et al.* Multilevel longitudinal analysis of shooting performance as a function of stress and cardiovascular responses. *IEEE Transactions on Affect. Comput.* **12**, 648–665, DOI: 10.1109/TAFFC.2020.2995769 (2021).

13. Kerick, S. E. *et al.* Neural and behavioral adaptations to frontal theta neurofeedback training. *PLoS ONE* (In Review).

14. Delignieres, D. *et al.* Fractal analyses for 'short' time series: A re-assessment of classical methods. *J. mathematical psychology* **50**, 525–544 (2006).

15. Turalska, M. & West, B. J. Fractional dynamics of individuals in complex networks. *Front. Phys.* **6**, DOI: 10.3389/fphy.2018.00110 (2018).

16. Manneville, P. Intermittency, self-similarity and 1/f spectrum in dissipative dynamical systems. *J. de Physique* **41**, 1235–1243 (1980).

17. Van Orden, G. C., Holden, J. G. & Turvey, M. T. Self-organization of cognitive performance. *J. Exp. Psychol. Gen.* **132**, 331–350, DOI: 10.1037/0096-3445.132.3.331 (2003).

18. Van Orden, G. C., Holden, J. G. & Turvey, M. T. Human cognition and 1/f scaling. *J. Exp. Psychol. Gen.* **134**, 117–123, DOI: 0.1037/0096-3445.134.1.117 (2005).

19. Peng, C. K., Havlin, S., Stanley, H. E. & Goldberger, A. L. Quantification of scaling exponents and crossover phenomena in nonstationary heartbeat time series. *Chaos* **5**, 82–87, DOI: 10.1063/1.166141 (1995).

20. Sokolov, I. Lévy flights from a continuous-time process. *Phys. Rev. E* **63**, 011104 (2000).

21. Scher, H. & Montroll, E. W. Anomalous transit-time dispersion in amorphous solids. *Phys. Rev. B* **12**, 2455 (1975).

22. Bologna, M. Distribution with a simple laplace transform and its applications to non-poissonian stochastic processes. *J. Stat. Mech. Theory Exp.* **2020**, 073201 (2020).

23. Ehrenstein, W. H. & Ehrenstein, A. *Psychophysical methods*, 1211–1241 (Springer Berlin Heidelberg, 1999).

24. Buiatti, M., Grigolini, P. & Palatella, L. A non extensive approach to the entropy of symbolic sequences. *Phys. A: Stat. Mech. its Appl.* **268**, 214–224 (1999).

25. Annunziato, M. & Grigolini, P. Stochastic versus dynamic approach to lévy statistics in the presence of an external perturbation. *Phys. Lett. A* **169**, 31–39 (2000).

26. Lukovic, M. & Grigolini, P. Power spectra for both interrupted and perennial aging processes. *J. Chem. Phys.* **129**, 184102–184113 (2008).

Acknowledgements

This study was supported by US Army Research Laboratory cooperative agreement W911NF-16-2-0008.

Author contributions statement

S.E.K. conceived and conducted the original experiment, K.M., P.G., and B.J.W conceived and applied the novel DFA analysis. All authors contributed to analyses of results and writing and reviewing the manuscript.

Competing interests

The authors declare no competing interests.